

Comparison of ^{64}Cu and ^{68}Ga for Molecular Imaging of Atherosclerosis using the Apolipoprotein A-I Mimetic Peptide FAMP

Eiji Yahiro^{1*}, Emi Kawachi^{1*}, Shin-Ichiro Miura^{1,2*}, Takashi Kuwano¹, Satoshi Imaizumi¹, Atsushi Iwata¹, Koki Hasegawa³, Tsuneo Yano^{4,5}, Yasuyoshi Watanabe⁶, Yoshinari Uehara^{1,2} and Keijiro Saku^{1,2*}

¹Department of Cardiology, Fukuoka University School of Medicine, Fukuoka, Japan

²Department of Molecular Cardiovascular Therapeutics, Fukuoka University School of Medicine, Fukuoka, Japan

³Department of Pathology and Experimental Medicine, Kumamoto University Graduate School of Medical Sciences, Kumamoto, Japan

⁴Engineering Department, Industrial Equipment Division, Sumitomo Heavy Industries Ltd., Japan

⁵Osaka University Graduate School of Medicine, Osaka, Japan

⁶RIKEN Center for Life Science Technologies, Kobe, Japan

*E.Y. and E.K. contributed equally to this work

Abstract

Background: Molecular imaging for detection of the atherosclerotic plaque burden has been highlighted as a modality for the diagnosis of atherosclerosis. We recently developed a novel and noninvasive positron emission tomography (PET) that was functionalized with an apolipoprotein (Apo) A-I mimetic peptide [known as Fukuoka University Apo A-I mimetic peptide (FAMP)] radiolabeled with gallium-68 (^{68}Ga) - 1, 4, 7, 10-tetraazacyclododecane-1, 4, 7, 10-tetraacetic acid (DOTA) to specifically image the status of atherosclerotic plaque in myocardial infarction-prone Watanabe heritable hyperlipidemic rabbits (WHHL-MI).

Methods and Results: To achieve more sensitive molecular imaging, FAMP was modified with 4, 11 - bis (carboxymethyl) - 1, 4, 8, 11 - tetraazabicyclo (6.6.2) hexadecane (CB-TE2A) and radiolabeled with copper-64 (^{64}Cu) for PET, and the ability of ^{64}Cu -TE2A-FAMP to image plaque was compared with that of ^{68}Ga -DOTA-FAMP. Japanese white normal (JW) and WHHL-MI rabbits were intravenously injected with ^{64}Cu -CB-TE2A-FAMP or ^{68}Ga -DOTA-FAMP, and subjected to continuous PET (25-30 MBq). Interestingly, ^{64}Cu -CB-TE2A-FAMP was not taken up by atherosclerotic lesions in the aorta of WHHL-MI, whereas ^{68}Ga -DOTA-FAMP was dramatically illuminated in the aorta of WHHL-MI. Moreover, ^{64}Cu -CB-TE2A-FAMP was rapidly decomposed and ^{64}Cu was excreted to the intestine, liver or urinary bladder in both JW and WHHL-MI rabbits.

Conclusions: These results demonstrated that FAMP may be a target molecule for atherosclerotic molecular imaging with ^{68}Ga -DOTA, but not with ^{64}Cu -CB-TE2A. The selection of a suitable radio-nuclide and chelator might be important for HDL functioning imaging.

Keywords: Molecular imaging; Positron emission tomography; Apolipoprotein A-I mimetic peptide; Watanabe heritable hyperlipidemic rabbits

Introduction

Cardiovascular disease is the leading cause of death in the world [1]. Atherosclerosis affects arterial blood vessels due to chronic inflammation and induces cardiovascular disease. Molecular imaging aims to identify and guide the treatment of vulnerable atherosclerotic plaque. A novel and noninvasive positron emission tomography (PET)-based method for imaging inflammatory plaque with ^{18}F -fluorodeoxyglucose (FDG) is currently of interest in the clinical setting [2]. Although atherosclerotic disease may produce no or only mild diffuse uptake along the vessel wall in FDG-PET, both the sensitivity and molecular specificity for targeting atherosclerosis by FDG-PET are relatively low [3-5].

Since the physical interactions between apolipoprotein A-I (Apo A-I) and ATP-binding cassette transporter 1 (ABCA1) modulate not only binding to Apo A-I but also internalization and transcytosis in macrophages and aortic endothelial cells, Apo A-I mimetic peptide may be a candidate for functional high-density lipoprotein (HDL) imaging in atherosclerosis. We recently synthesized a novel 24-amino acid Apo A-I mimetic peptide without phospholipids [known as Fukuoka University Apo A-I mimetic peptide (FAMP)], which potently removes cholesterol *in vitro* via specific ABCA1 [6]. In that study using a cholesterol-fed mouse model, we found that

FAMP promoted macrophage reverse cholesterol transport (RCT). Moreover, we demonstrated that the unique Apo A-I mimetic peptide FAMP with gallium-68 (^{68}Ga) - 1, 4, 7, 10-tetraazacyclododecane-1, 4, 7, 10-tetraacetic acid (DOTA) is a promising candidate diagnostic tracer for imaging the atherosclerotic lipid burden [7]. Nonetheless, molecular imaging using ^{68}Ga -DOTA-FAMP may not be enough for detecting the atherosclerotic burden clearly because ^{68}Ga has a short physical half-life (68 min).

The aim of the present study was to achieve more sensitive molecular imaging in atherosclerotic lesions. Therefore, FAMP was modified with 4, 11 - bis (carboxymethyl) - 1, 4, 8, 11 - tetraazabicyclo (6.6.2) hexadecane (CB-TE2A) and radiolabeled with copper-64 (^{64}Cu) for PET, since ^{64}Cu has a relatively long physical half-life (12.7 h), and

*Corresponding author: Shin-ichiro Miura and Keijiro Saku, Department of Cardiology, Fukuoka University School of Medicine, 7-45-1 Nanakuma, Jonan-ku, Fukuoka, 814-0180, Japan, Tel: 81-92-801-1011; Fax: 81-91-865-2692; E-mail: miuras@cis.fukuoka-u.ac.jp; saku-k@fukuoka-u.ac.jp

Received April 22, 2015; Accepted May 25, 2015; Published May 27, 2015

Citation: Yahiro E, Kawachi E, Miura SI, Kuwano T, Imaizumi S, et al. (2015) Comparison of ^{64}Cu and ^{68}Ga for Molecular Imaging of Atherosclerosis using the Apolipoprotein A-I Mimetic Peptide FAMP. J Cardiovasc Dis Diagn 3: 201. doi:10.4172/2329-9517.1000201

Copyright: © 2015 Yahiro E, et al. This is an open-access article distributed under the terms of the Creative Commons Attribution License, which permits unrestricted use, distribution, and reproduction in any medium, provided the original author and source are credited.

molecular imaging using ^{64}Cu -CB-TE2A-FAMP was compared with that using ^{68}Ga -DOTA-FAMP.

Methods

Synthesis of CB-TE2A-FAMP and DOTA-FAMP

FAMP (H-ALEHLFTLYEKALKALEDLLKLL-OH) was modified with CB-TE2A (Macrocyclics, Dallas, TX, USA) (Figure 1A) and DOTA (Strem Chemicals Inc., Newburyport, MA, USA). To a solution of O - (1H-benzotriazol-1-yl) - N, N, N', N' - tetramethyluronium hexafluorophosphate (HBTU, 50 μmol) and 1-hydroxybenzotriazole (HOBt, 50 μmol) in N, N - dimethylformamide (DMF, 2 ml) were added CB-TE2A (50 μmol) and DIEA (N, N - diisopropylethylamine) 34 μL , and the mixture was stirred at room temperature. After several minutes, this solution was added to 50 $\mu\text{mol/L}$ FAMP resin and stirred at room temperature for 1 hour. The resulting CB-TE2A-FAMP resin was deprotected with a TFA mixture that contained triisopropylsilane (1.0%), 1, 2-ethanedithiol (2.5%) and water (2.5%) for 2 h. After deprotection, cold diethyl ether was added to the mixture, and the precipitate was collected by centrifugation. Obtained crude CB-TE2A-FAMP was purified by reversed-phase high-performance liquid chromatography (HPLC). Purified CB-TE2A-FAMP was

analyzed by matrix-assisted laser desorption/ionization time-of-flight mass spectrometry (MALDI-TOF MS; found: m/z 3,137.2 ($M+H$) $^+$, calculated for ($M+H$) $^+$: 3,137.8) (Figure 1B). DOTA-N-hydroxysuccinimidyl (NHS) ester was prepared by the preferential activation of 1 carboxyl group of the DOTA chelator in dimethyl sulfoxide (DMSO), as described previously [7,8].

Radiolabeling of ^{64}Cu -CB-TE2A-FAMP and ^{68}Ga -DOTA-FAMP

CB-TE2A-FAMP and DOTA-FAMP were radiolabeled with ^{64}Cu and ^{68}Ga , respectively, for use in noninvasive PET imaging. Cu-64 was produced by proton-irradiation of a ^{64}Ni electroplated gold disc target using a HM-12S cyclotron (Sumitomo Heavy Industries, Ltd., Tokyo, Japan) [9]. The crude Cu-64 was dissolved in 6 N HCl and purified manually on an ion exchange resin (DOWEX 1X8 100-200 mesh; Muromachi Technos Co., Ltd., Tokyo, Japan) to produce (^{64}Cu) CuCl_2 . ^{68}Ga -DOTA-FAMP was prepared using the method described previously [7,10].

Animals

We purchased Japanese white (JW) rabbits from Japan SLC Inc. (Shizuoka, Japan). In addition, myocardial infarction-prone

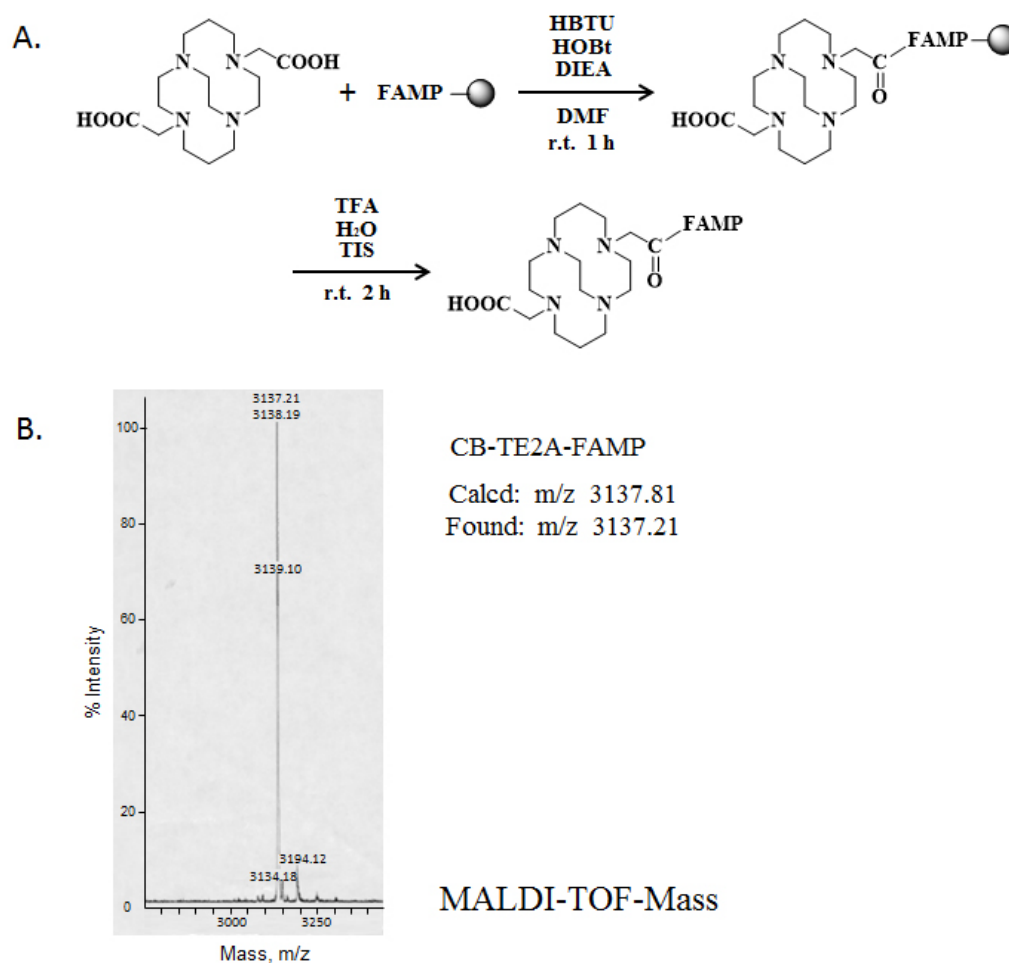


Figure 1: A) Scheme for the preparation of 4, 11 - bis (carboxymethyl) - 1, 4, 8, 11 - tetraazabicyclo [6.6.2] hexadecane-Fukuoka University Apo A-I mimetic peptide (CB-TE2A-FAMP). B) DOTA-FAMP was separated by reversed-phase high-performance liquid chromatography and analyzed by matrix-assisted laser desorption/ionization time-of-flight mass spectrometry (found: m/z 3137.21 ($M+H$) $^+$, calculated for ($M+H$) $^+$: 3137.81).

homozygous Watanabe heritable hyperlipidemic (WHHL-MI) rabbits with total cholesterol >700 mg/dl were provided by Dr Shiomi, Kobe University, Japan. The rabbits were injected with ^{64}Cu -CB-TE2A-FAMP (2 nmol per animal) and ^{68}Ga -DOTA-FAMP (2-5 nmol per animal). The rabbits were maintained at Fukuoka University, Japan, and experiments were performed at the RIKEN Center for Molecular Imaging Science, Japan. The experiments complied with the regulations of the Committee on Ethics in the Care and Use of Laboratory Animals. The rabbits were housed in rooms maintained at $23 \pm 1^\circ\text{C}$ and $55 \pm 5\%$ relative humidity with free access to water and standard diet during acclimatization, and were fasted for 24 hr before PET imaging.

PET imaging protocol

Imaging was carried out using a microPETR Focus220 (Siemens, Knoxville, TN, USA) as described previously [7]. Briefly, emission data acquisition was started at the same time as the intravenous administration of ^{64}Cu -CB-TE2A-FAMP and ^{68}Ga -DOTA-FAMP for 6 h with an energy window of 400-650 keV and a coincidence timing window of 6 ns. The emission images were reconstructed by using filtered back projection with a Ramp filter and a cutoff at the Nyquist frequency. The time course of ^{64}Cu activity in the region of the abdominal aortic bifurcation was obtained using ASIPro software included with the microPET system, and the results were adjusted for the background.

Results

Time-dependent attenuation of ^{64}Cu -CB-TE2A-FAMP at the abdominal aortic bifurcation

We performed a PET analysis 6 h after the injection of ^{64}Cu -CB-TE2A-FAMP at the abdominal aortic bifurcation, when radioactivity should be completely cleared from the circulation. PET images of the abdominal aorta revealed little accumulation of ^{64}Cu -CB-TE2A-FAMP in either JW or WHHL-MI rabbits (Figure 2). The time-dependent attenuation of ^{64}Cu -CB-TE2A-FAMP in the abdominal aortic bifurcation in WHHL-MI rabbits was mild compared with that in JW rabbits.

PET imaging after injection of the tracer

PET images clearly showed a high uptake of the ^{68}Ga -DOTA-FAMP tracer in the aorta of WHHL-MI rabbits (Figure 3A), and little uptake in the aorta of JW rabbits (Figure 3B). On the other hand, PET images showed little uptake of ^{64}Cu -CB-TE2A-FAMP in the aorta of either WHHL-MI or JW rabbits (Figure 3C, 3D). Furthermore, the clear uptake of ^{64}Cu -CB-TE2A-FAMP in the intestine, liver and bladder was seen in both WHHL-MI and JW rabbits (Figures 3C, 3D and 4A). Finally, there were no uptake in the aorta and the clear uptake of ^{64}Cu -CB-TE2A-FAMP in the intestine, liver and bladder at 24 h after the injection in both WHHL-MI and JW rabbits (Figure 4B, 4C).

Discussion

We previously developed a novel PET tracer, Apo A-I mimetic

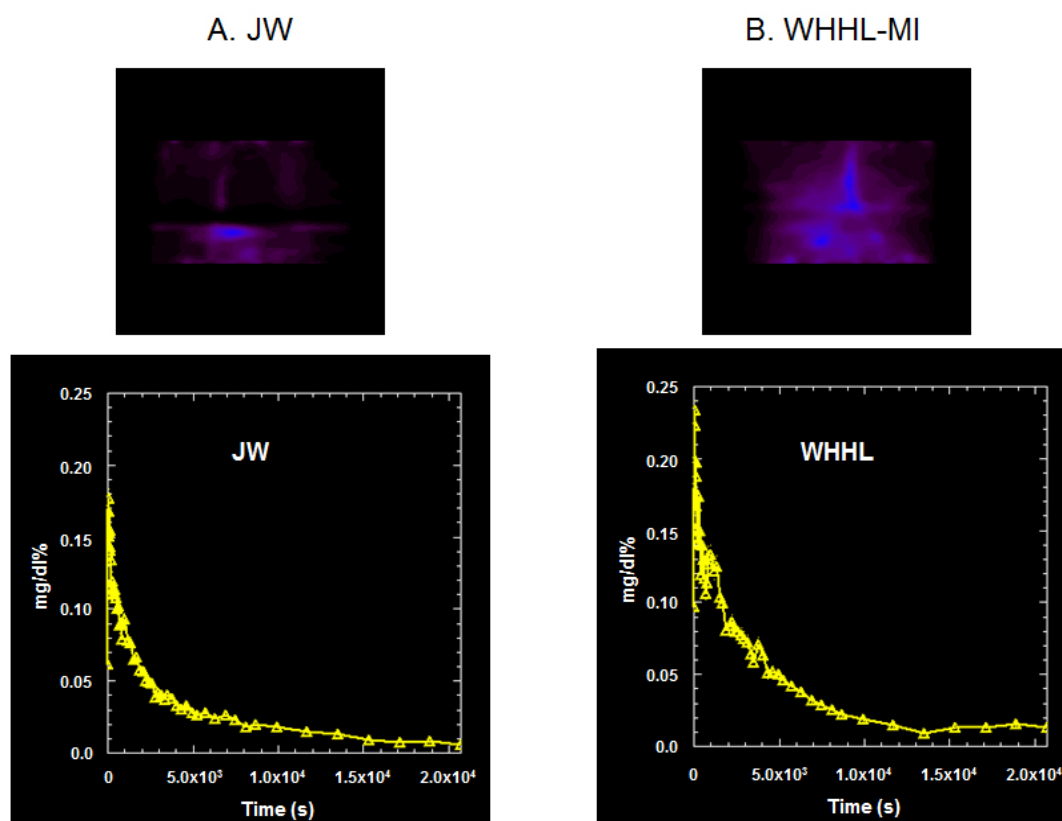


Figure 2: (A) Time-dependent attenuation of ^{64}Cu -CB-TE2A-FAMP at the abdominal aortic bifurcation in Japanese white (JW) and (B) myocardial infarction-prone homozygous Watanabe heritable hyperlipidemic (WHHL-MI) rabbits. Upper panels show continuous images of the abdominal aortic bifurcation for 6 h after the injection of tracers. ^{64}Cu -CB-TE2A, 4, 11 - bis (carboxymethyl) - 1, 4, 8, 11 - tetraazabicyclo [6.6.2] hexadecane; FAMP, Fukuoka University Apo A-I mimetic peptide.

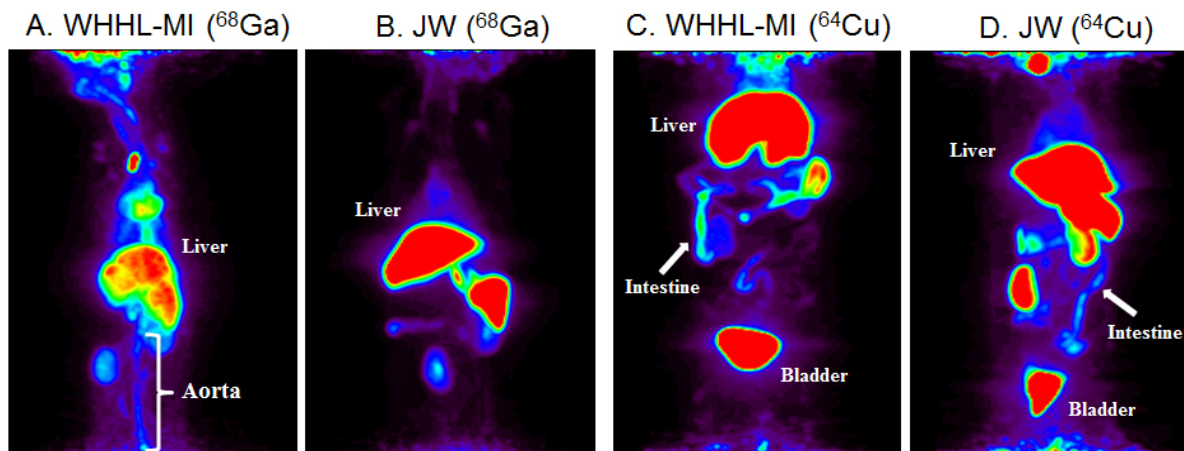


Figure 3: Positron emission tomography (PET) imaging after injection of the tracer reveals a high uptake of the ^{68}Ga -DOTA-FAMP tracer at 1.5 h after injection in the aorta of Watanabe heritable hyperlipidemic (WHHL-MI) rabbits (A), and no uptake of ^{68}Ga -DOTA-FAMP at 2 h after injection in the aorta of Japanese white (JW) rabbits (B). PET images showed no uptake of ^{64}Cu -CB-TE2A-FAMP at 6 h after injection in the aorta of both WHHL-MI (C) and JW rabbits (D). ^{68}Ga -DOTA, gallium-68-1,4,7,10-tetraazacyclododecane-1,4,7,10-tetraacetic acid; ^{64}Cu -CB-TE2A, 4, 11 - bis (carboxymethyl) - 1, 4, 8, 11 - tetraazabicyclo [6.6.2] hexadecane; FAMP, Fukuoka University Apo A-I mimetic peptide.

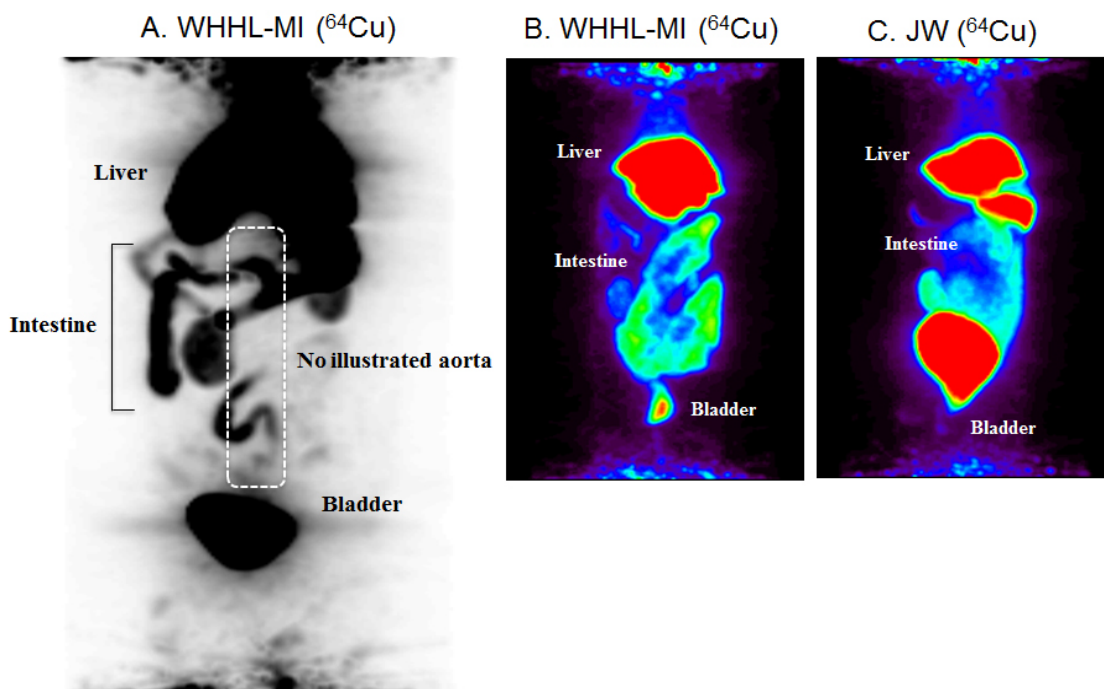


Figure 4: Positron emission tomography (PET) imaging at 6 h after injection of the tracer reveals a high uptake of ^{64}Cu -CB-TE2A-FAMP tracer in the intestine, liver and bladder of Watanabe heritable hyperlipidemic (WHHL-MI) rabbits (A). PET imaging at 24 h after injection of the tracer reveals a high uptake of ^{64}Cu -CB-TE2A-FAMP tracer in the intestine, liver and bladder of WHHL-MI (B) and Japanese white (JW) rabbits (C).

peptide FAMP radiolabeled with ^{68}Ga -DOTA, to specifically image the status of atherosclerotic plaque in WHHL-MI [7]. To achieve more sensitive molecular imaging, FAMP was modified with CB-TE2A and radiolabeled with ^{64}Cu for PET, and the ability of ^{64}Cu -TE2A-FAMP to image plaque was compared with that of ^{68}Ga -DOTA-FAMP. ^{68}Ga -DOTA-FAMP was interestingly superior to ^{64}Cu -CB-TE2A-FAMP in atherosclerotic molecular imaging. The selection of a suitable radionuclide and chelator should be important for HDL functioning imaging.

In this study, we selected ^{64}Cu as a tracer because it has a longer half-life than ^{68}Ga (12.7 h and 68 min, respectively) for more feasibility clinical use. The half-life of fluorescence-labeled FAMP in blood was about 4 h, according to data on blood clearance of FAMP in mice [6]. Although we thought that a combination of ^{64}Cu and FAMP could provide superior molecular imaging, PET images showed no uptake of ^{64}Cu -CB-TE2A-FAMP in the aorta at 6 h after injection (Figure 3C). Since we did not observe any uptake of ^{64}Cu -CB-TE2A-FAMP in the aorta at 1-2 h after injection (data not shown), we consider that ^{64}Cu -

CB-TE2A-FAMP did not provide HDL-functional imaging. Instead, ⁶⁴Cu-CB-TE2A-FAMP may be rapidly decomposed, since ⁶⁴Cu was excreted to the intestine, liver or urinary bladder in both JW and WHHL-MI rabbits (Figures 3CD and 4A). Previous reports have shown that ⁶⁴Cu-DOTA and ⁶⁴Cu-TETA complex are moderately unstable in vivo due to the release of uncoordinated ⁶⁴Cu by decomposition in the blood or transchelation in the liver, which leads to high uptake in non-target tissues [11,12]. ⁶⁴Cu-labeled DOTA/TETA conjugates often show poor blood and liver clearance, high uptake in non-target organs, and increased background radioactivity levels, resulting in reduced imaging sensitivity [13,14]. As for ⁶⁴Cu-CB-TE2A complexes, Sprague et al. indicated that the ⁶⁴Cu-CB-TE2A-Tyr3-octreotate shows improved blood, liver, and kidney clearance compared with the analogous ⁶⁴Cu-TETA agent [15]. ⁶⁴Cu-CB-TE2A-c is a potential candidate for imaging tumor angiogenesis [16]. In addition, ⁶⁴Cu-CB-TE2A-ReCCMSH(Arg11) also showed greatly improved liver and blood clearance as well as higher tumor-to-non-target tissue ratios compared with ⁶⁴Cu-DOTA-ReCCMSH (Arg11) [17]. Thus, many researchers have successfully performed molecular imaging using ⁶⁴Cu-CB-TE2A. We do not know why ⁶⁴Cu-CB-TE2A-FAMP may be rapidly decomposed in vivo at this stage, although we successfully synthesized and purified ⁶⁴Cu-CB-TE2A-FAMP as shown in Figure 1. Further studies are needed to solve this issue.

Although ⁶⁸Ga-DOTA-FAMP was interestingly superior to ⁶⁴Cu-CB-TE2A-FAMP for atherosclerotic molecular imaging, the PET images obtained with ⁶⁸Ga-DOTA-FAMP tracer show atherosclerotic plaques more clearly than those obtained using previously reported tracers (¹⁸F-FDG and ¹¹¹In-low-density lipoprotein, etc.) [18-20]. FAMP has been shown to have a high capacity for cholesterol efflux from A172 cells and mouse and human macrophages *in vitro*, and this efflux was mainly dependent on ABCA1 transporter [6]. ⁶⁸Ga-DOTA-FAMP may accumulate in atherosclerotic plaque, which requires FAMP. Mizoguchi et al. reported that a pioglitazone-treated group demonstrated significantly greater suppression of FDG imaging of carotid and aortic plaque inflammation compared with a glimepiride group in patients with diabetes mellitus [21]. Their study only found a decrease in inflammation after treatment, and could not assess changes in plaque volume or vulnerability. In addition, the precise mechanisms that underlie FDG uptake in atheroma are not clear. Recently, Santulli et al. proposed an innovative strategy based on a selective microRNA in the treatment of atherosclerosis and restenosis [22]. Since the final aim of molecular imaging is to identify and guide the treatment of vulnerable atherosclerotic plaques that are at high risk of rupture and subsequent thrombosis, we need to identify a better strategy for achieving more sensitive and specific molecular imaging using FAMP in the future.

There are several study limitations in this study. First, it is important to match PET-positive lesions with the results of immunohistochemical analysis to determine the cell make-up, although we did not perform the analysis because of the difficulties associated with radioactive tissue. Second, the target molecule for ⁶⁸Ga-DOTA-FAMP has not yet been identified. Third, PET imaging cannot include the heart, we targeted the descending aorta (bifurcation of aorta) and could not perform coronary imaging.

In conclusion, these results demonstrated that FAMP may be a target molecule for atherosclerotic molecular imaging with ⁶⁸Ga-DOTA, but not with ⁶⁴Cu-CB-TE2A. The selection of a suitable radionuclide and chelator might be important for HDL functioning imaging.

Acknowledgements

None.

Funding

This work was supported by grants-in-aid from the Ministry of Education, Science and Culture of Japan (No. 21590960, No. 24591123), the Fukuoka University One-Campus Project (2009, 2010, supported in part by the Ministry of Education, Science and Culture of Japan), a grant-in-aid from the AIG Collaborative Research Institute of Cardiovascular Medicine, Fukuoka University, Japan, and NPO Clinical and Applied Science, Fukuoka, Japan.

K.S. is a Chief Director and S.M. is a Director of NPO Clinical and Applied Science, Fukuoka, Japan. K.S. has an Endowed "Department of Molecular Cardiovascular Therapeutics" supported by MSD, Co. LTD. S.M. and Y.U. belong to the Department of Molecular Cardiovascular Therapeutics, which is supported by MSD, Co. LTD.

References

1. Santulli G (2013) Epidemiology of cardiovascular disease in the 21st century: updated numbers and updated facts. J Cardiovasc Dis 1:1-2.
2. Osborn EA, Jaffer FA2 (2013) The advancing clinical impact of molecular imaging in CVD. JACC Cardiovasc Imaging 6: 1327-1341.
3. Miyagawa M, Yokoyama R, Nishiyama Y, Ogimoto A, Higaki J, et al. (2014) Positron emission tomography-computed tomography for imaging of inflammatory cardiovascular diseases. Circ J 78: 1302-1310.
4. Rudd JH, Myers KS, Bansilal S, Machac J, Woodward M, et al. (2009) Relationships among regional arterial inflammation, calcification, risk factors, and biomarkers: A prospective fluorodeoxyglucose positron-emission tomography/computed tomography imaging study. Circ Cardiovasc Imaging 2: 107-115.
5. Rudd JH, Warburton EA, Fryer TD, Jones HA, Clark JC, et al. (2002) Imaging atherosclerotic plaque inflammation with [18F]-fluorodeoxyglucose positron emission tomography. Circulation 105: 2708-2711.
6. Uehara Y, Ando S, Yahiro E, Oniki K, Ayaori M, et al. (2013) FAMP, a novel apoA-I mimetic peptide, suppresses aortic plaque formation through promotion of biological HDL function in ApoE-deficient mice. J Am Heart Assoc 2: e000048.
7. Kawachi E, Uehara Y, Hasegawa K, Yahiro E, Ando S, et al. (2013) Novel molecular imaging of atherosclerosis with gallium-68-labeled apolipoprotein A-I mimetic peptide and positron emission tomography. Circ J 77: 1482-1489.
8. Kamei N, Morishita M, Kanayama Y, Hasegawa K, Nishimura M, et al. (2010) Molecular imaging analysis of intestinal insulin absorption boosted by cell-penetrating peptides by using positron emission tomography. J Control Release 146: 16-22.
9. McCarthy DW, Shefer RE, Klinkowstein RE, Bass LA, Margeneau WH, et al. (1997) Efficient production of high specific activity ⁶⁴Cu using a biomedical cyclotron. Nucl Med Biol 24: 35-43.
10. Zhemosekov KP, Filosofov DV, Baum RP, Aschoff P, Bihl H, et al. (2007) Processing of generator-produced ⁶⁸Ga for medical application. J Nucl Med 48: 1741-1748.
11. Boswell CA, Sun X, Niu W, Weisman GR, Wong EH, et al. (2004) Comparative in vivo stability of copper-64-labeled cross-bridged and conventional tetraazamacrocyclic complexes. J Med Chem 47: 1465-1474.
12. Sun X, Wuest M, Weisman GR, Wong EH, Reed DP, et al. (2002) Radiolabeling and in vivo behavior of copper-64-labeled cross-bridged cyclam ligands. J Med Chem 45: 469-477.
13. Anderson CJ, Jones LA, Bass LA, Sherman EL, McCarthy DW, et al. (1998) Radiotherapy, toxicity and dosimetry of copper-64-TETA-octreotide in tumor-bearing rats. J Nucl Med 39: 1944-1951.
14. McQuade P, Miao Y, Yoo J, Quinn TP, Welch MJ, et al. (2005) Imaging of melanoma using ⁶⁴Cu- and ⁸⁶Y-DOTA-ReCCMSH(Arg11), a cyclized peptide analogue of alpha-MSH. J Med Chem 48: 2985-2992.
15. Sprague JE, Peng Y, Sun X, Weisman GR, Wong EH, et al. (2004) Preparation and biological evaluation of copper-64-labeled tyr3-octreotate using a cross-bridged macrocyclic chelator. Clin Cancer Res 10: 8674-8682.

16. Wei L, Ye Y, Wadas TJ, Lewis JS, Welch MJ, et al. (2009) (64)Cu-labeled CB-TE2A and diamsar-conjugated RGD peptide analogs for targeting angiogenesis: comparison of their biological activity. *Nucl Med Biol* 36: 277-285.
17. Wei L, Butcher C, Miao Y, Gallazzi F, Quinn TP, et al. (2007) Synthesis and biologic evaluation of 64Cu-labeled rhenium-cyclized alpha-MSH peptide analog using a cross-bridged cyclam chelator. *J Nucl Med* 48: 64-72.
18. Pedersen SF, Græbe M, Hag AM, Højgaard L, Sillesen H, et al. (2013) (18) F-FDG imaging of human atherosclerotic carotid plaques reflects gene expression of the key hypoxia marker HIF-1 α . *Am J Nucl Med Mol Imaging* 3: 384-392.
19. Noh TS, Moon SH, Cho YS, Hong SP, Lee EJ, et al. (2013) Relation of carotid artery 18F-FDG uptake to C-reactive protein and Framingham risk score in a large cohort of asymptomatic adults. *J Nucl Med* 54: 2070-2076.
20. Rosen JM, Butler SP, Meinken GE, Wang TS, Ramakrishnan R, et al. (1990) Indium-111-labeled LDL: a potential agent for imaging atherosclerotic disease and lipoprotein biodistribution. *J Nucl Med* 31: 343-350.
21. Mizoguchi M, Tahara N, Tahara A, Nitta Y, Kodama N, et al. (2011) Pioglitazone attenuates atherosclerotic plaque inflammation in patients with impaired glucose tolerance or diabetes a prospective, randomized, comparator-controlled study using serial FDG PET/CT imaging study of carotid artery and ascending aorta. *JACC Cardiovasc Imaging* 4: 1110-1118.
22. Santulli G, Wronska A, Uryu K, Diacovo TG, Gao M, et al. (2014) A selective microRNA-based strategy inhibits restenosis while preserving endothelial function. *J Clin Invest* 124: 4102-4114.